‘Ghost’ Silica Nanoparticles of ‘Host’-Inherited Antibacterial Action

Ahmed F. Halbus,[a,b] Tommy S. Horozov,[a] Vesselin N. Paunov*[a]

[a] Department of Chemistry and Biochemistry, University of Hull, Hull HU6 7RX, U.K.

[b] Department of Chemistry, College of Science, University of Babylon, Hilla, IRAQ.

KEYWORDS copper oxide nanoparticles, silica nanoparticles, mesoporous particles, templating, surface roughness, antibacterial nanoparticles, boronic acid, bacteria.

ABSTRACT: We fabricated surface-rough mesoporous silica nanoparticles (‘ghost’ SiO_2NPs) by using composite mesoporous copper oxide nanoparticles (‘host’ CuONPs) as templates which allowed to copy their surface morphology. The ‘host’ CuONPs used here as templates, however, had a very high antibacterial effect, with or without functionalization. In order to evaluate the surface roughness effect on the ‘ghost’ SiO_2NPs antibacterial action we functionalized them with (3-glycidyloxypropyl)trimethoxysilane (GLYMO) to permit additional covalent coupling of 4-hydroxyphenylboronic acid (4-HPBA). The diol groups on the bacterial membrane can form reversible covalent bonds with boronic acid (BA) groups on the ‘ghost’ SiO_2NPs surface and bind to the bacteria, causing in a very strong amplification of their antibacterial activity which does not depend on electrostatic adhesion. The BA-functionalized ‘ghost’ SiO_2NPs showed a very significant antibacterial effect compared to smooth SiO_2NPs of the same surface coating and particle size. We attribute this to the ‘ghost’ SiO_2NPs mesoporous surface morphology which mimics to certain extend those of the original mesoporous CuONPs used as templates for their preparation. We envisage that the ‘ghost’ SiO_2NPs effectively acquires some of the antibacterial properties from the ‘host’ CuONPs, with the same functionality, despite being completely free of copper. The antibacterial effect of the functionalized ‘ghost’ SiO_2NPs/GLYMO/4-HPBA on *Rhodococcus rhodochrous* (*R.rhodochrous*) and *Escherichia coli* (*E.coli*) is much higher than that of the non-functionalized ‘ghost’ SiO_2NPs or the ‘ghost’ SiO_2NPs/GLYMO. The results indicate that the combination of rough surface morphology and strong adhesion of the particle surface to the bacteria can make even benign material as silica act as a strong antimicrobial agent. Additionally, our BA-functionalized nanoparticles (‘ghost’ SiO_2NPs/GLYMO/4-HPBA) showed no detectable cytotoxic impact against human keratinocytes at particle concentrations which are effective against bacteria.

INTRODUCTION

Nanoparticles have been extensively explored for a range of biomedical applications, as contrast agents for medical imaging, labelling of cells, targeting of tumors and therapeutic drug delivery.[1-2,65] The optical, photoactive, electronic, catalytic and thermal properties can be greatly influenced by the specific particle morphology (sphere, cube, rod, etc.) and size.[3-5] Often the nanoparticle shape and size can be easily controlled with a high degree of accuracy during their synthesis procedure.[6-15] Nanoparticles have been heavily researched in recent years for their potential nanotoxicity and promising antimicrobial capabilities due to their high surface area to volume ratios,[16-19] and nanoparticles of different metal oxides[20] as titanium dioxide,[21] zinc oxide[22] iron oxides[23] silver and copper oxides[24],[64] have been investigated. Antibacterial action includes the disruption of the bacterial membrane integrity leading to the leakage of intracellular components [25], creation of reactive oxygen species (ROS) harming bacterial cell constituents[24] as well as metal ions leaching from the nanoparticles interfering with the metabolism of the bacteria.[26] These mechanisms are found to rely on the particle shape, size, surface charge, chemical functionalities and composition.[27-35]

SiO_2NPs have been explored as good candidates for drug delivery vehicles, biosensor applications and biomedical imaging due to their relatively low toxicity against mammalian cells, their biocompatibility and their easy surface modifications.[36-37] SiO_2NPs modified with either photosensitizing molecules or antibiotics, or anchored to hybrid materials are promising in both bacterial detection[38] and antibacterial action.[39] Despite this great potential, the effects of the surface morphology of SiO_2NPs on the interactions with bacteria are not well documented in the literature.[32] SBA-15 mesoporous silica sieve with uniform hexagonal pores, a narrow pore size distribution and a tunable pore diameter of between 5 and 15 nm have been used by Molina-Manso and co-workers to encapsulate 3 various antimicrobial agents such as rifampicin, linezolid and vancomycin.[40] Yu *et al.* have studied the use of poly(N-isopropylacrylamide)-gated Fe_3O_4/SiO_2 core shell nanoparticles for the temperature triggered release of antibacterial enzyme lysozyme.[41] Ruiz-Rico and others have stated the antimicrobial effect of caprylic acid incorporated in mesoporous silica particles against *Escherichia coli*, *Salmonella enterica*, *Staphylococcus aureus* and *Listeria monocytogenes*. They discovered that bacteria treatment with the caprylic acid-loaded silica nanoparticles produced disruption of cell envelope and leakage of cytoplasmic content, which resulted in cell death.[42] Design and synthesis of surface-rough nanoparticles have attracted much attention due to their special structure and wide applications.[43]

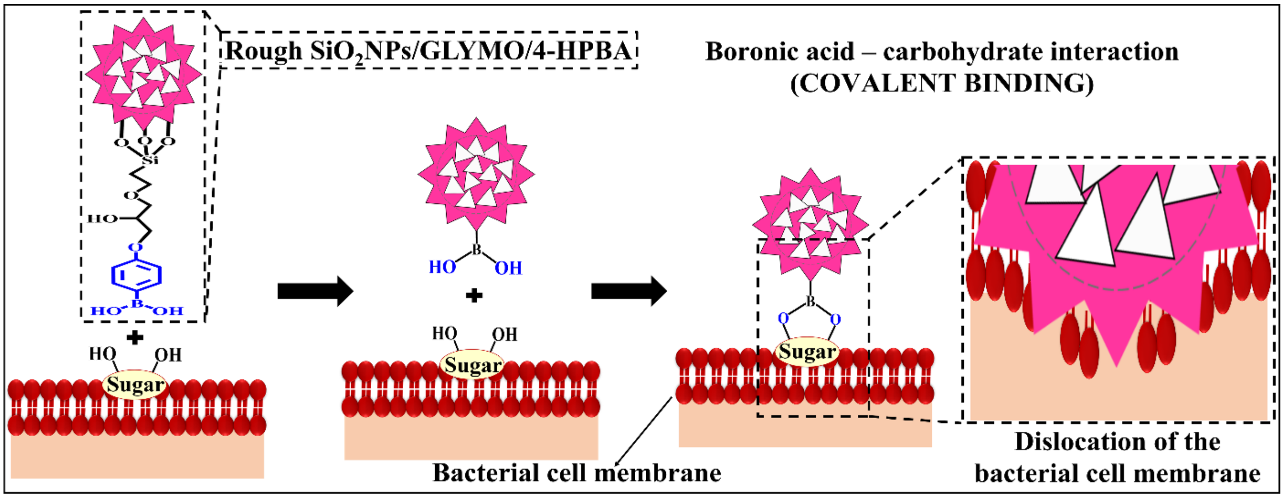

Figure 1. Schematics displaying the mechanism of self-grafting/covalent binding of the sugar groups expressed on the bacterial cell wall and boronic acid-functionalized surface-rough SiO_2NPs ('ghost').

Here we explore the role of the silica particle surface roughness on their antimicrobial action. We prepared the surface-rough SiO_2NPs by using mesoporous shaped CuONPs as templates (host), which are reported to have strong antimicrobial action.[2,63,64] In order to explore the effect of the particle surface roughness and morphology we effectively created 'ghost' SiO_2NPs which copy the morphology of the templated 'host' CuONPs. The CuO was removed from the composite CuO/SiO2 nanoparticles by dissolving the CuO with nitric acid and additional cleaning with EDTA which left mesoporous SiO_2NPs with similar size and morphology as the host nanoparticle but free of any copper content. However, since the original CuONP is positive charged at pH 7 and normally attach to the negatively charged bacteria, we needed to engineer a similar attraction between bacteria and the rough and mesoporous 'ghost' SiO_2NPs. For this reason, we functionalized the 'ghost' SiO_2NPs with BA-surface groups in attempt to design a non-electrostatic binding mechanism to the bacterial cell wall which is expected to accumulate them on the bacterial cell surface even in the presence of other anionic species in the aqueous solution. The BA-groups on the surface-rough SiO_2NPs are able to covalently attach to different carbohydrates and glycoproteins that are expressed on the bacterial membrane surfaces. BA-functionality has been utilized before in chemosensor applications because of its high sensitivity for sugar determination[44] and the antimicrobial properties of BA-functionalized CuONPs particles have been recently reported.[2,63,64] The BA-surface functionalization of the SiO_2NPs was done using GLYMO and further conjugation of phenylboronic acid.[2,63,64] An attractive property of the BA-surface functionality that makes it very active for biomedical applications is its perceived lack of toxicity[45] in spite of its ability to form reversible covalent binding with diol groups.[46-47] Attachment of BA to sugars is sensitive to the sugar concentration, nevertheless, it is non-discriminating and will thus attach to any diol containing compounds.[48] BA has been utilized as a promising material for the evaluation of the total content of bacteria.[49-51] Saccharides can covalently attach to BA groups and form boronic esters.[2, 52-54,63,64] For comparison, we used smooth SiO_2NPs of similar size surface functionalized in the same way as the 'ghost' SiO_2NPs/GLYMO/4-HPBA in order to compare their antibacterial action and evaluate the effect of the particle surface roughness. This is shown schematically in Figure 1.

We studied the antibacterial action of the 4-HPBA functionalized smooth and rough SiO2NPs on *R.rhodochrous* and *E.coli* as representative Gram-positive and Gram-negative bacterial species, respectively. The present study was carried out with SiO_2NPs, SiO_2NPs/GLYMO and SiO_2NPs/GLYMO/4-HPBA to examine the antibacterial effect as a function of the NPs concentration, the zeta potential and particle size on the cell viability of bacteria at different exposure times. Importantly, the functionalization of the rough SiO_2NPs with BA surface groups should lead to their covalent binding on the saccharides containing diol groups on the bacterial cell membrane, therefore impaling their rough SiO_2NPs on the bacteria cells which can potentially break up the membrane and increase the antibacterial effect.

MATERIALS AND METHODS

Materials

R.rhodochrous was provided from Blades Biological, UK (Carolina.com, item No. 155175). *E.coli*, obtained from Thermofisher (Invitrogen MAX Efficiency DH10B), was kindly supplied for our antibacterial tests by Prof. J. Rotchell's group at the Hull University, U.K. We used NaOH (99.6%, Fisher Scientific, UK) with $CuCl_2$ (99%, Sigma Aldrich) as a precursor in the preparation of CuONPs by the direct precipitation method.

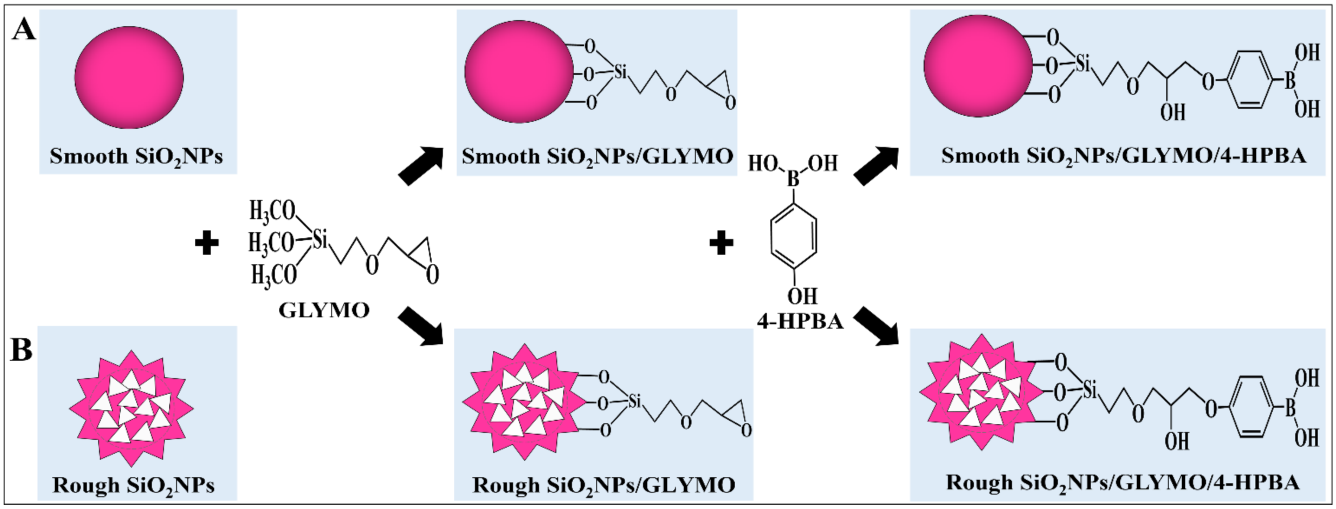

Figure 2. A schematic of the synthesis method of (A) a surface-smooth SiO_2NPs/GLYMO/4-HPBA and (B) a surface-rough SiO_2NPs/GLYMO/4-HPBA by sequential grafting of GLYMO and 4-HPBA on SiO_2NPs in an aqueous suspension.

Ammonia solution (35 %, 1.2 mL), Tetraethyl orthosilicate (TEOS), Ethylenediaminetetraacetic acid (EDTA), Fluorescein diacetate (FDA), GLYMO and 4-HPBA were sourced from Sigma Aldrich. BacTiter-Glo (BTG) microbial cell viability assay was supplied by Promega, UK. The silica nanoparticles with smooth surface and a nominal diameter of 100 nm were obtained from Fiber Optical Center, USA. Deionized water purified by ion exchange and reverse osmosis with a Milli-Q system (Millipore, UK) was utilized in this work. At 25°C its surface tension was 71.9 mNm^{-1}, with measured resistivity exceeding 18 $M\Omega\ cm^{-1}$.

Methods

Surface coating of CuONPs with SiO_2. The silica-coated copper oxide nanoparticles labelled as CuONPs/SiO_2 were prepared. The method is similar to the SiO_2 functionalization of other NPs, [55-56] but in our manuscript, the porous CuONPs were further modified with SiO_2. 0.1 g of CuONPs was dispersed in a mixture of concentrated NH_3 solution (35 %, 1.2 mL), ethanol (40 mL) and deionized water (10 mL) by ultrasonication for 1 h. To the above mixture, TEOS (0.43 mL) was added dropwise. After stirring for 6 h, the mixture was collected and washed with ethanol and deionized water.[57] Similar version of this procedure and the antibacterial tests with the resulting particles are described in the ESI, where instead of 1.2 mL 35% ammonia solution, 0.1 g of sodium hydroxide (99.6% purity) is used as a catalyst.

Surface modification of CuONPs/SiO_2 by GLYMO and 4-HPBA. 0.1 wt% of GLYMO were added to the suspension of CuONPs/SiO_2, followed by stirring for 1 h. The reaction mixture was stirred for 1 day, then washed three times with deionized water by centrifugation to remove the excess of GLYMO. The procedure is similar to the APTES functionalization of other inorganic NPs [58] but in our work GLYMO brings epoxy-ring as a terminal group. No other study in the present literature has reported such functionality as this was done here for the first time. The CuONPs/SiO_2/GLYMO was then redispersed in 100 mL of deionized water and added dropwise to 0.1 g of 4-HPBA dissolved in 100 mL of ethanol. After being shaken for 2 h, the samples were washed three times with ethanol by centrifugation for 30 min at 10000 rpm. Finally, the formed CuONPs/SiO_2/GLYMO/4-HPBA were redispersed in 100 mL of deionized water.[2, 59-61]

Surface modification of smooth SiO_2NPs by GLYMO and 4-HPBA. 0.1 g of smooth SiO_2NPs were dispersed in 100 mL of deionized water at pH 7. Then, the same procedure used in the surface modification of CuONPs/SiO_2 described above was followed. The SiO_2NPs/GLYMO/4-HPBA were re-dispersed in 100 mL of deionized water.[2, 59-61] Figure 2 shows the chemistry of the process of surface functionalization of both smooth and rough SiO_2NPs with 4-HPBA.

Synthesis of surface rough 'ghost' SiO_2NPs. The rough SiO_2NPs were prepared by using CuONPs as templates ('host' particles). CuONPs were first synthesized in aqueous solution. Silica was then deposited on the nano-porous CuONPs to achieve CuONPs/SiO_2 nanostructures using ammonia solution as a catalyst (labelled as rough SiO_2NPs) or NaOH as a catalyst (labelled as rough SiO_2NPs-2 – see ESI). The synthesized CuONPs/SiO_2 nanoparticles were isolated from the suspension by centrifugation. Further, they were treated with 1M HNO_3. After 24 h, the resulting SiO2NPs were centrifuged, washed with EDTA and deionized water to remove completely the Cu^{2+} ions, producing rough and mesoporous 'ghost' SiO_2NPs as shown in Figure 3. The rough 'ghost' SiO_2NPs were further modified with GLYMO and 4-HPBA by similar procedures as reported above.

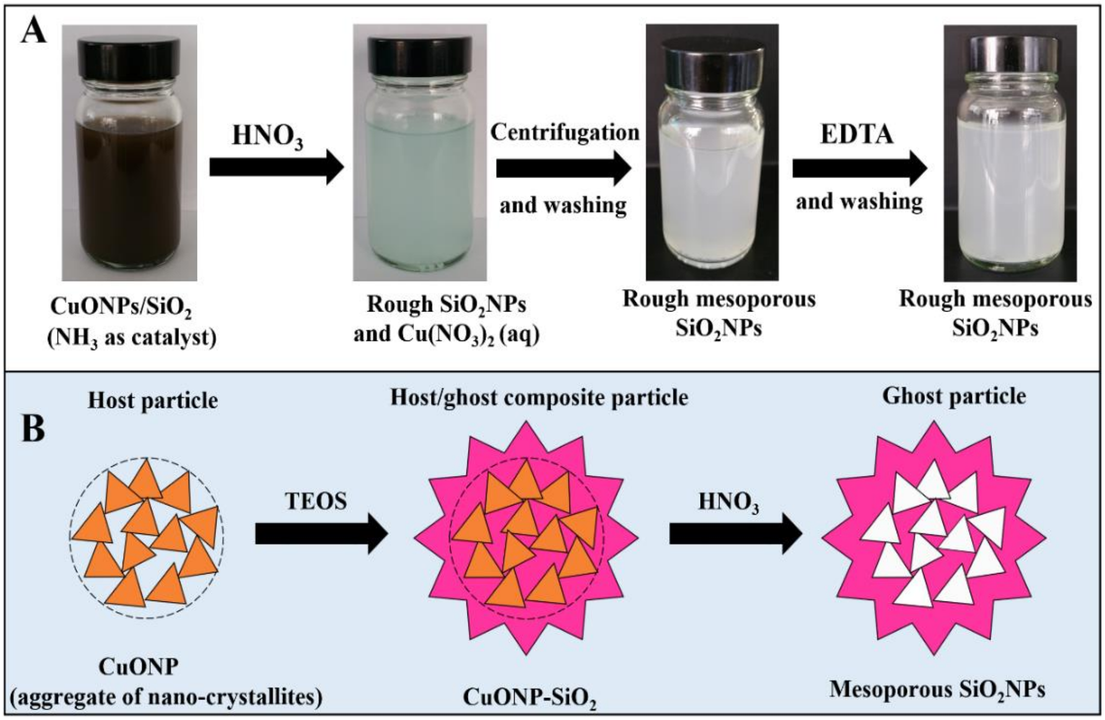

Figure 3. Schematics showing the synthesis of (A) a surface-rough SiO_2NPs (NH_4OH as a catalyst) and (B) the schematic of the synthesis method of CuONPs/SiO_2 (host/ghost composite particles) and surface-rough SiO_2NPs (ghost particles) from CuONPs (host particles).

Antibacterial action of bare and BA-surface functionalized SiO_2NPs on bacteria. The culture media of *R.rhodochrous* was prepared by adding 13 g of nutrient broth to 1 L of deionized water. It was mixed well and transferred into the final containers after autoclaving at 125°C and 1.5 bar for 1 h. Once the culture media was cooled down to 30 °C, a few microliters of the stock solution of *R.rhodochrous* were dispersed in the autoclaved culture media beside the Bunsen burner. The *R.rhodochrous* was incubated with shaking at 30 °C for 5-7 days. The *R.rhodochrous* were removed from their growth media and transferred in deionized water. Non-functionalized and HPBA-functionalized SiO_2NPs were incubated with fixed aliquots of the *R.rhodochrous* cultures for various incubation times. Then, 1 mL aliquot of each *R.rhodochrous* suspension was washed with deionized water by centrifugation and re-suspended in 1 mL deionized water to yield starting concentrations in the range of (0.5–1.0) × 10^6 colony forming units per mL (CFU/mL). 100 μL of BacTiter-Glo™ cell viability reagent was mixed with 100 μL of the treated *R.rhodochrous* suspension in a white opaque 96-well microplate and shaken for 5 min. The bioluminescence intensity was then measured as a function of the incubation time and used to determine the fraction of viable *R.rhodochrous* upon exposure to different concentrations of BA-surface functionalized SiO_2NPs. Non-functionalized SiO_2NPs were used as an additional control.

Cell viability of HaCaT cells treated with bare SiO_2NPs and HPBA-functionalized SiO_2NPs. HaCaT cells (an immortalised human keratinocyte cell line, sourced from the Skin Research Group at St James University Hospital at Leeds) were cultured in DMEM supplemented with 1% L-glutamine and 10% FBS under humidified conditions at 5% CO_2, 37°C in T75 flasks until a confluency of 70% was reached, determined by visualisation with an optical microscope. The cells were accurately washed with PBS for 10 sec then incubated with 1× trypsin buffer at 37 °C 5% CO_2 for 5 min until the cells were detached into the suspension. The trypsin was neutralized by adding fresh DMEM media before a centrifugation for 4 min at 400g. The HaCaT cells culture (~75000 cells mL^{-1}) were removed from their growth media by centrifugation and transferred in 25 mL PBS. Then, the non-functionalized and the HPBA-functionalized SiO_2NPs at different concentrations were incubated with fixed aliquots of the HaCaT cells suspension for various incubation times.

The HaCaT cells without exposure to any nanoparticles (a control sample) were kept at identical conditions. The viability of HaCaT cells suspension was measured using a microplate reader after incubating 1 mL of the treated HaCaT cells (washed from the non-functionalized or HPBA-functionalized SiO_2NPs), with 10 μL of 0.1% FDA in acetone for 15 min and washing with PBS by centrifugation for 4 min at 400g. The HaCaT cell viability test was repeated in three independent experiments.

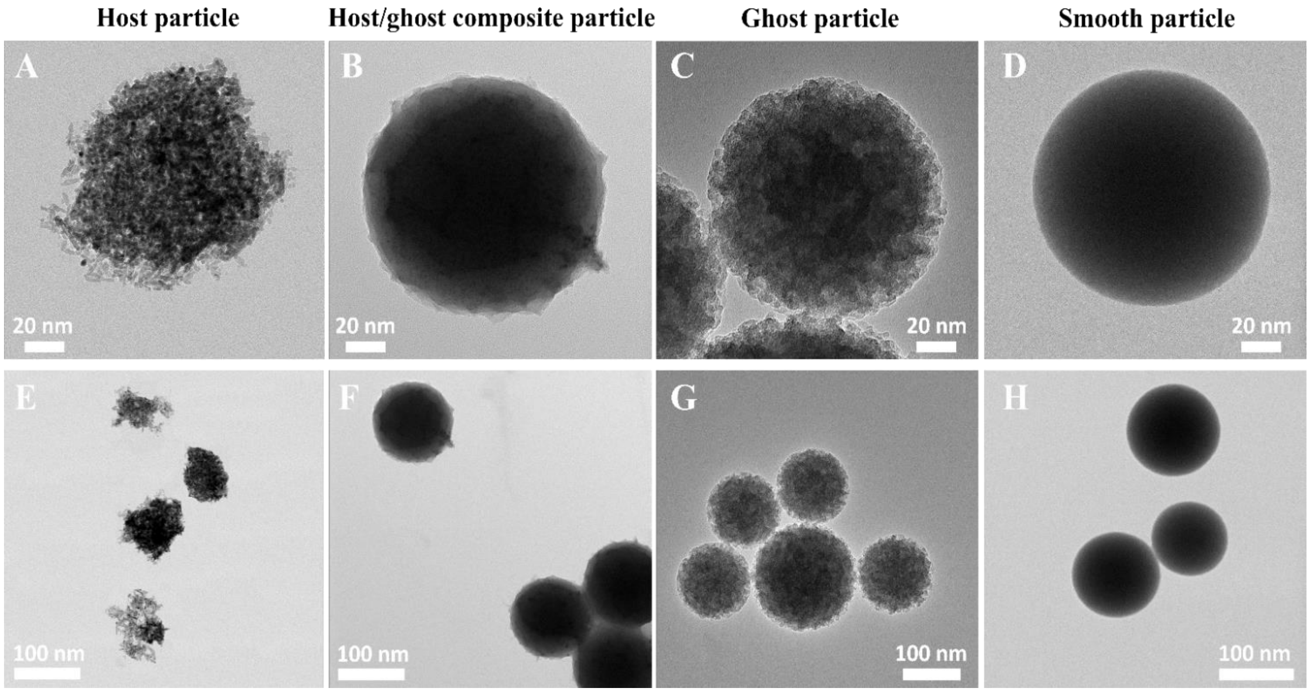

Figure 4. TEM images of (A,E) bare CuONPs which are aggregates of nano-crystallites (host) , (B,F) SiO_2-coated CuONPs producing a surface-rough SiO_2NPs (host/ghost composite particles), (C,G) mesoporous surface-rough 'ghost' SiO_2NPs, (D, H) smooth SiO_2NPs of very similar particle size.

TEM imaging of the treated bacteria. After incubation with non-functionalized and HPBA-functionalized NPs, the *R.rhodochrous* cells were visualized by TEM imaging using the following protocol. The cells were washed with deionized water 3 times to remove the residual NPs by centrifugation at 500g for 5 min and then fixed in 2 wt% glutaraldehyde at room temperature for 1 h, followed by washing with cacodylate buffer. The *R.rhodochrous* were post fixed for 1 h in 1 wt% osmium tetroxide, washed with a cacodylate buffer. The bacteria were incubated for 1 h with 2.5 wt% uranyl acetate and washed with aqueous ethanol solutions of increasing ethanol concentration. After standard dehydration, the bacteria were embedded in fresh epoxy/Araldite resin for 48 h at 60 °C, left at room temperature for 48 h and then sectioned with an ultra-microtome and finally imaged using TEM.

RESULTS AND DISCUSSION

Surface modification of CuONPs with SiO_2, GLYMO and 4-HPBA. Figures 4A and 4E show the TEM images of the CuONPs formed by using the process with annealing at 100 °C and further sonication in deionized water. SiO_2-coated copper oxide nanoparticles were synthesized using base-catalyzed hydrolysis (with ammonia solution) of tetraethyl orthosilicate in the presence of CuONPs. A typical TEM image of the obtained CuONPs/SiO_2 (Figures 4B, 4F) showed that the cluster-shaped copper nanoparticles (darker) were infused and coated with a uniform silica (light gray) - see also Figure S1A and S1B (ESI). The average hydrodynamic diameter of the CuONPs/SiO_2 measured by dynamic light scattering has increased in comparison to the core CuONPs, corresponding to a 25 ± 5 nm thick SiO_2 deposited layer, and the surface of the (host/ghost) composite CuONPs/SiO_2 became rough as the deposited silica follows the topology of the rough CuONPs surface. These nanoparticles were treated with HNO_3 solution to remove the CuONPs ('host') templates completely, producing mesoporous and surface rough 'ghost' SiO_2NPs as shown in Figure 4C, which copies certain surface roughness features from the original host particles. The zeta potential of the nanoparticles has also changed from a positive value of +37 ± 3 mV for the bare CuONPs to a negative value of - 44 ± 7 mV after their surface modification with a SiO_2 layer, GLYMO and 4-HPBA as shown in Figure S2A (ESI). The negative surface charge of silica contributed to the reduction in the total charge of the composite 'host/ghost' nanoparticles. Dynamic light scattering analysis indicated that the size of the CuONPs has slightly increased after coating with SiO_2 and the subsequent functionalization with GLYMO and 4-HPBA (Figure S2B (ESI)).

Surface modification of the mesoporous surface-rough SiO_2NPs. The rough SiO_2NPs (ghost NPs) were prepared by using the CuONPs (host NPs) as templates. CuONPs were first synthesized in aqueous solution, silica layer was then deposited on the CuONPs to yield composite CuONPs/SiO_2 nanoparticles.

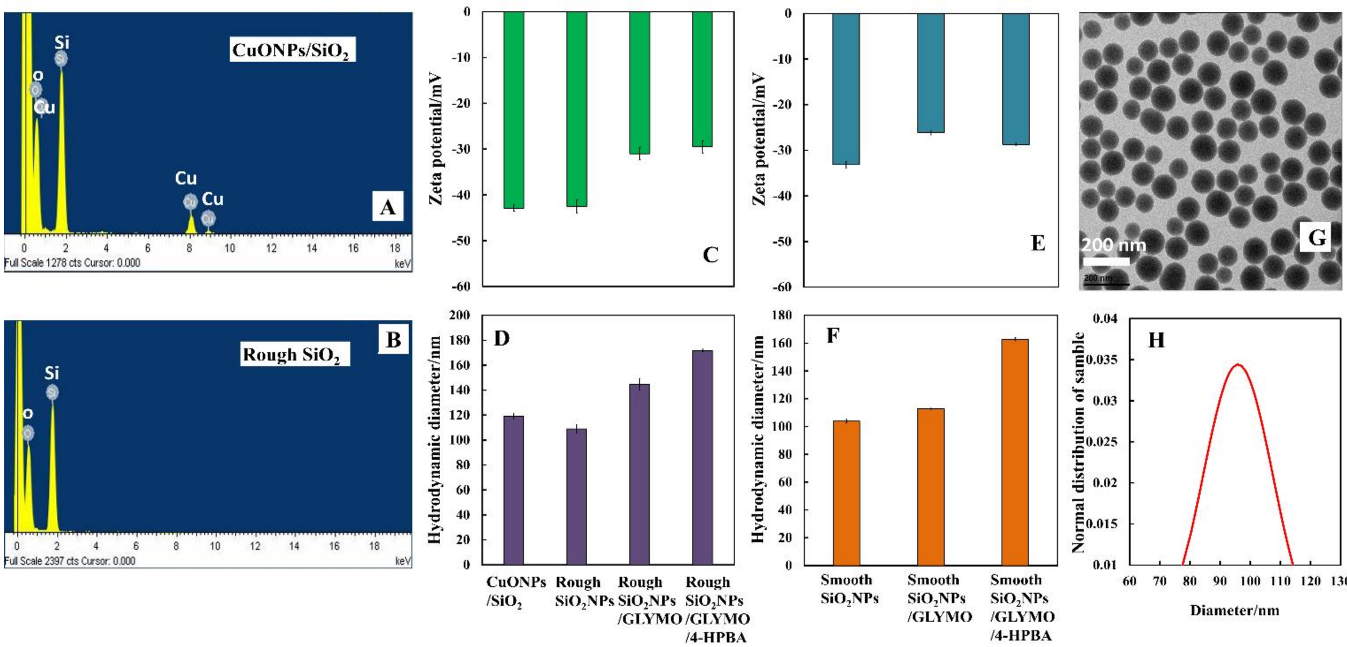

Figure 5. EDX spectrum of the CuONPs/SiO_2 nanoparticles before (A) and after (B) treatment with HNO_3 and EDTA solution. (C) The zeta potential and (D) the particle hydrodynamic diameter of the composite CuONPs/SiO_2, the rough SiO_2NPs, the rough SiO_2NPs/GLYMO and the rough SiO_2NPs/GLYMO/4-HPBA at pH 7. (E) The zeta potential and (F) the particle hydrodynamic diameter of smooth SiO_2NPs, SiO_2NPs/GLYMO and SiO_2NPs/GLYMO/4-HPBA at pH 7. (G) TEM image of the smooth SiO_2NPs and (H) their size distribution.

The composite CuONPs/SiO_2 were dispersed in the HNO_3 and EDTA solution to remove any traces of CuO and copper ions from the produced rough SiO_2NPs. Figure 4C and 4D show the TEM images of the resultant surface-rough SiO_2NPs and an analogous surface smooth SiO_2NPs obtained from Fiber Optical Center (USA), respectively. The images in Figure 4A and 4C shows that the rough surface morphology of the original CuONPs clusters is reflected in the produced rough SiO_2NPs. Thus, rough SiO2NPs with the size of 115 ± 10 nm was successfully fabricated from CuONPs. Figure S1C and S1D (ESI) showing the TEM images of a surface-rough SiO_2NPs at different magnifications confirm that the particles produced with NaOH catalyst in the Stöber process have similar morphology and roughness to those prepared with ammonia as a catalyst. Figure 5A and 5B shows EDX analysis of the CuONPs/SiO_2 nanoparticles before and after treatment with HNO_3 and EDTA solution. Figure 5A shows the presence of Cu, Si and O before the treatment as expected. However, the EDX spectrum of the silica after treatment with HNO_3 (Figure 5B) shows only two main peaks for Si and O components with no peaks of copper. Hence the 'ghost' SiO_2NPs are free of copper oxide and Cu^{2+} residues. Since they have negative surface charge, one could expect them not to have antimicrobial action. The surface-rough SiO_2NPs were modified by GLYMO and 4-HPBA and further characterized using DLS measurements. The data in Figure 5C and Figure S3A (ESI) show that the zeta potentials of the bare rough SiO_2NPs and rough SiO_2NPs/GLYMO/4-HPBA are both negative, similar to the negatively charged bacterial cell membranes. The hydrodynamic diameter of the bare rough SiO_2NPs was 115 ± 10 nm, whereas that of the rough SiO_2NPs/GLYMO and rough SiO_2NPs/GLYMO/4-HPBA was slightly larger, as shown in Figure 5D and Figure S3B (ESI).

Surface modification of smooth SiO_2NPs by GLYMO and 4-HPBA. At first, the smooth silica nanoparticles were dispersed in deionized water, then, functionalized with GLYMO needed for the subsequent grafting of 4-phenylboronic acid. The GLYMO is expected to attach to the silica surface by reaction between the hydroxyl and silanol groups followed by an easy reaction between the epoxy group of GLYMO and hydroxyl groups of 4-HPBA. Figure 5G shows TEM images of smooth SiO_2NPs before the functionalizing process. DLS measurements made by using a Malvern Zetasizer Nano ZS system have shown that the smooth SiO_2NPs have fairly narrow diameter distribution (Figure 5H). The average diameter of the bare smooth SiO_2NPs is 107 ± 10 nm, which is consistent with the TEM result shown in Figure 5F. The zeta potential of smooth SiO_2NPs slightly changed after modification with GLYMO and 4-HPBA (Figure 5E) but remained negative.

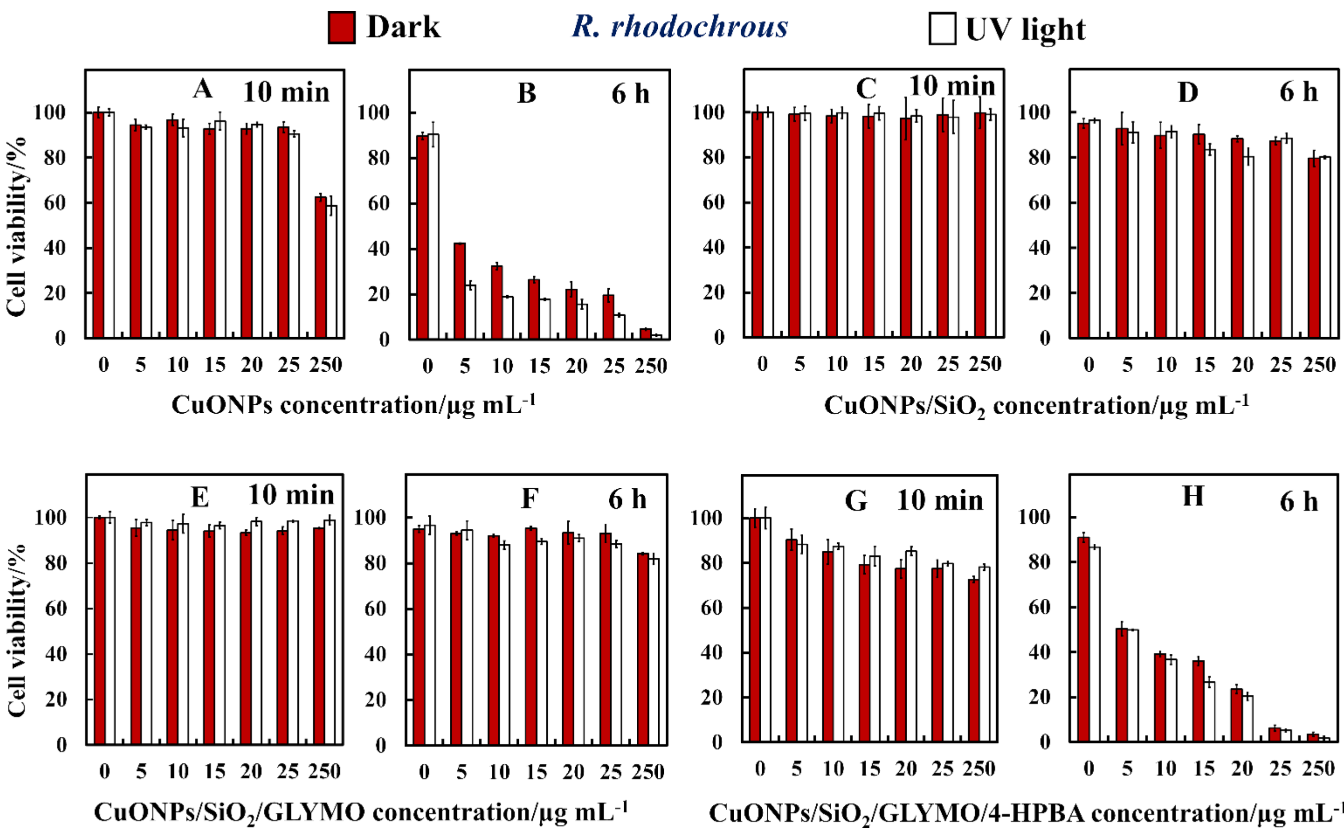

Figure 6. The effect of free and surface functionalized CuONPs of various particle concentrations on the viability of *R.rhodochrous* upon incubation in UV light and dark conditions. The bacteria cells were incubated with: (A, B) non-functionalized CuONPs; (C, D) SiO_2-functionalized CuONPs, (E, F) GLYMO, SiO_2-functionalized CuONPs and (G, H) HPBA, GLYMO, SiO_2-functionalized CuONPs at 10 min and 6 h exposure times.

Antibacterial action of CuONPs/SiO_2 surface functionalized by GLYMO and 4-HPBA. Figure 6 displays the antibacterial impact of suspensions of bare CuONPs, composite CuONPs/SiO_2, CuONPs/SiO_2/GLYMO and CuONPs/SiO_2/GLYMO/4-HPBA of various particle concentrations on *R.rhodochrous*. In this case (Figure 6), the CuONPs crystallites are still inside the composite NPs and have not yet been removed. We also functionalized these particles with GLYMO and 4-HPBA to study their antibacterial action. The data in Figure 6 indicate that the bare CuONPs have an extremely strong antibacterial impact in a wide range of concentrations ranged from 5 µg mL^{-1} to 250 µg mL^{-1} after 6 h of incubation (see Figure 6B). Figure 6D and 6F show the antibacterial impact of the CuONPs/SiO_2 and CuONPs/SiO_2/GLYMO on *R.rhodochrous* after 6 h incubation time at room temperature. In this case, there was no pronounced antibacterial impact upon the incubation of *R.rhodochrous* with each individual concentration. The antibacterial effect of CuONPs/SiO_2 and CuONPs/SiO_2/GLYMO in dark conditions and under UV light is much lower than the one of the bare CuONPs. One may conclude that the functionalization of the CuONPs with SiO_2 and subsequently with GLYMO reduced their antibacterial effect. This is probably due to the electrostatic repulsion of the CuONPs/SiO_2 and the functionalized CuONPs/SiO_2/GLYMO from the *R.rhodochrous* surface as both the particles and cell membranes have a negative surface charge. However, after functionalizing these nanoparticles with 4-HPBA (CuONPs/SiO_2/GLYMO/4-HPBA), the viability of the *R.rhodochrous* was considerably reduced as shown in Figure 6G and 6H. In fact, their antibacterial effect is similar to that of the bare CuONPs. This could be explained by the boronic acid functionality in CuONPs/SiO_2/GLYMO/4-HPBA which can selectively bind with carbohydrates expressed on the bacteria surface by covalent interactions. TEM imaging confirmed that the outer cell walls of bacteria accumulate a significant number of deposited non-modified CuONPs (Figure 7B) and CuONPs/SiO_2/GLYMO/4-HPBA (Figure 7E and 7F) over 6 h of incubation. In contrast, the bacterial cells exposed to CuONPs/SiO_2 (Figure 7C) and CuONPs/SiO_2/GLYMO (Figure 7D) show smooth and intact bacteria membranes similar to those untreated with nanoparticles (Figure 7A). The results in Figure 7E and 7F shows TEM images of the bacteria incubated with HPBA- and GLYMO-functionalized CuONPs/SiO_2. One can see that there is a significant impact of this functionality in promoting the adhesion to the surface of the cell walls.

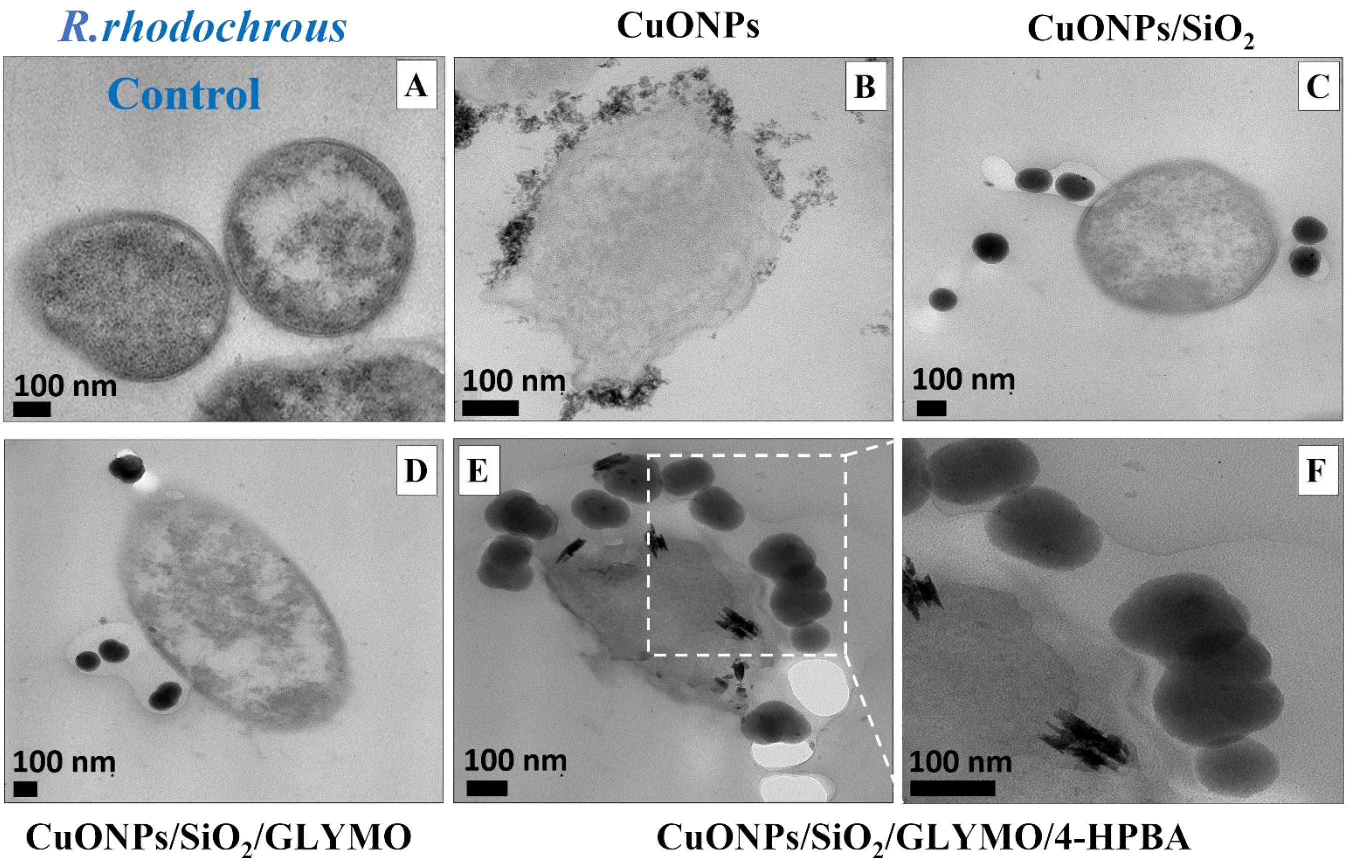

Figure 7. TEM images of 25 µg mL^{-1} free and surface functionalized CuONPs after being incubated for 6 h with *R.rhodochrous*: (A) represent the control sample (untreated); (B) sample incubated with free CuONPs; (C) sample incubated with CuONPs/SiO_2; (D) sample incubated with GLYMO, CuONPs/SiO_2, and (E, F) sample incubated with HPBA, GLYMO, CuONPs/SiO_2.

The strong covalent interaction of the HPBA-functionalized CuONPs/SiO_2 with the cell walls is probable the main contributor towards bacterial walls disruption and damage which makes it a very effective antibacterial agent.

Antibacterial activity of surface functionalized smooth SiO_2NPs against *R.rhodochrous*. Antibacterial activity experiments were conducted through the incubation of suspensions of various particle concentrations of smooth SiO_2NPs, smooth SiO_2NPs/GLYMO and smooth SiO_2NPs/GLYMO/4-HPBA with *R.rhodochrous.* The data in Figure 8A-8D show a very low antibacterial activity on *R.rhodochrous* upon incubation with series of suspensions of various particle concentrations of bare SiO_2NPs, SiO_2NPs/GLYMO and SiO_2NPs/GLYMO/4-HPBA at room temperature. At 6-24 h exposure time, the percentage of *R.rhodochrous* viability was reduced in the case of smooth SiO_2NPs/GLYMO/4-HPBA particles at concentrations in the range 25-2000 µg mL^{-1}. In contrast, the *R.rhodochrous* viability with bare SiO_2NPs and SiO_2NPs/GLYMO was higher than that for SiO_2NPs/GLYMO/4-HPBA for the same particle concentrations and exposure times. These results indicate that a surface-smooth silica nanoparticles (see Figure 4D and 4D) do not apparently affect the viability of *R.rhodochrous* for the duration of these incubation experiments.

Antibacterial activity of surface functionalized rough SiO_2NPs and smooth SiO_2NPs on *R.rhodochrous*. We studied the viability of the bacterial cells after treatment with surface functionalized rough SiO_2NPs produced using two different catalysts, NH_4OH (or NaOH, see ESI), in the Stöber process, respectively. Figure 8E-8H compares the effect of the bare rough SiO_2NPs and the surface-functionalized rough SiO_2NPs with GLYMO and 4-HPBA at different particle concentrations on the *R.rhodochrous* viability. The functionalized 'ghost' SiO_2NPs particles in this experiment were produced using NH_4OH as catalyst. We incubated samples of *R.rhodochrous* with dispersions of rough SiO_2NPs (bare and functionalized with GLYMO and GLYMO/4-HPBA) at fixed particle concentrations (0, 25, 250, 500, 1000 and 2000 µg mL^{-1}) for different periods of exposure up to 24 h. The data in Figure 8E-8H reveal that no measurable change in the *R.rhodochrous* cell viability was observed for both rough SiO_2NPs and rough SiO_2NPs/GLYMO at 250 µg mL^{-1} particle concentrations. We did not detect significant difference between the rough SiO_2NPs and rough SiO_2NPs/GLYMO at the same particle concentration.

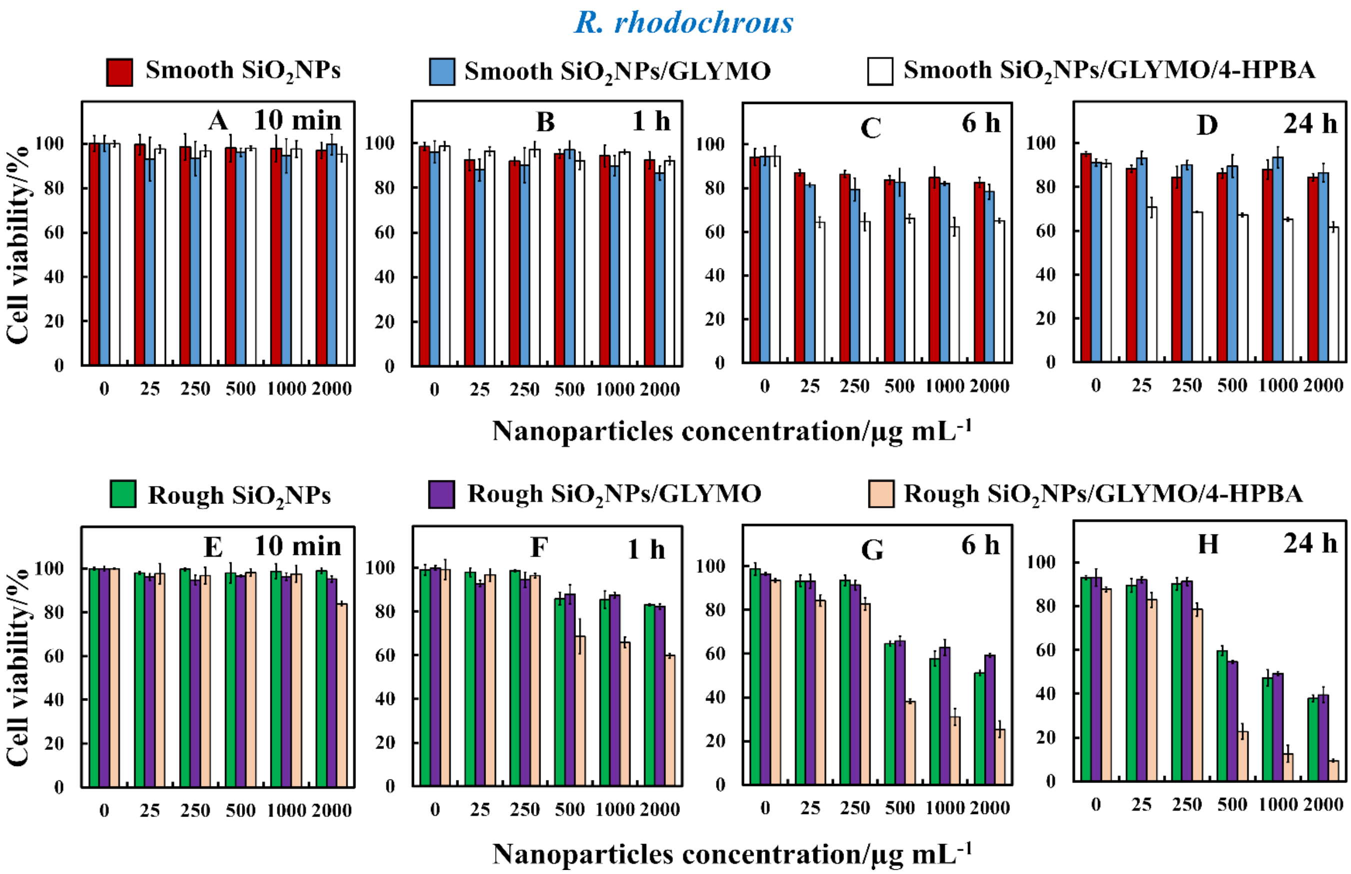

Figure 8. Cell viability of *R.rhodochrous* as a function of nanoparticle concentration with (A-D) smooth SiO_2NPs, SiO_2NPs/GLYMO and SiO_2NPs/GLYMO/4-HPBA. (E-H) 'Ghost' SiO_2NPs, 'ghost' SiO_2NPs/GLYMO and 'ghost' SiO_2NPs/GLYMO/4-HPBA of various particle concentrations. The incubation times were (A, E) 10 min, (B, F) 1 h, (C, G) 6 h and (D, H) 24 h, respectively.

For longer incubations times, however, the rough SiO_2NPs/GLYMO/4-HPBA showed significant antibacterial activity on *R.rhodochrous* at 500, 1000, 2000 µg mL^{-1} particle concentrations (Figure 8F-8H). We also tested the antibacterial activity of 4-HPBA-functionalized rough SiO_2NPs (made with NaOH as a catalyst) on *R.rhodochrous* as shown in Figure S4 (ESI). The data in Figure S4 (ESI) show similar antibacterial trends to those observed with rough SiO_2NPs prepared with ammonia as a catalyst (Figure 8E-8H). They also show that the rough SiO_2NPs/GLYMO/4-HPBA has a strong antibacterial effect on *R.rhodochrous* at 2000 µg mL^{-1} particle concentration. A plausible explanation for this result is that the surface morphology of the rough SiO_2NPs/GLYMO/4-HPBA forces the cell membrane of the bacteria to closely follow its topology due to formation of covalent bonds between the cis-diols groups on the cell membrane surface and the 4-hydroxyphenylboronic acid terminal groups on the particle surface. The adhesion of the rough nanoparticles to the cells due to formation of strong reversible boronic esters with carbohydrates and glycoproteins molecules which are abundant on the *R.rhodochrous* cell wall leads to dislocation of the bacterial membrane which kills the bacteria. Note also, that the free GLYMO or 4-HPBA reagents did not show any antibacterial activity at concentrations up to 2000 µg mL^{-1} (see Figure S5, ESI).

We compared the antibacterial activity of both bare (non-functionalized) and surface functionalized smooth and rough SiO_2NPs with GLYMO and 4-HPBA on *R.rhodochrous* in order to determine whether the surface roughness of the 'ghost' SiO_2NPs, that mimics the one of the original 'host' CuONPs, could enhance their antibacterial activity. Figure 9 compares the *R.rhodochrous* cell viability upon incubation with GLYMO/4-HPBA-functionalized SiO_2NPs and bare SiO_2NPs with the same nanoparticle concentration. The GLYMO/4-HPBA-functionalized 'ghost' SiO_2NPs shows much higher antibacterial efficiency against *R.rhodochrous* than both the bare 'ghost' SiO_2NPs and GLYMO-functionalized 'ghost' SiO_2NPs at the same conditions. The reason behind this is the rough surface morphology of the 'ghost' SiO_2NPs which upon covalent bonding between the rough SiO_2NPs/GLYMO/4-HPBA and the bacterial cell membrane causes its impaling on the surface rough features and produces membrane dislocation which kills the bacteria.

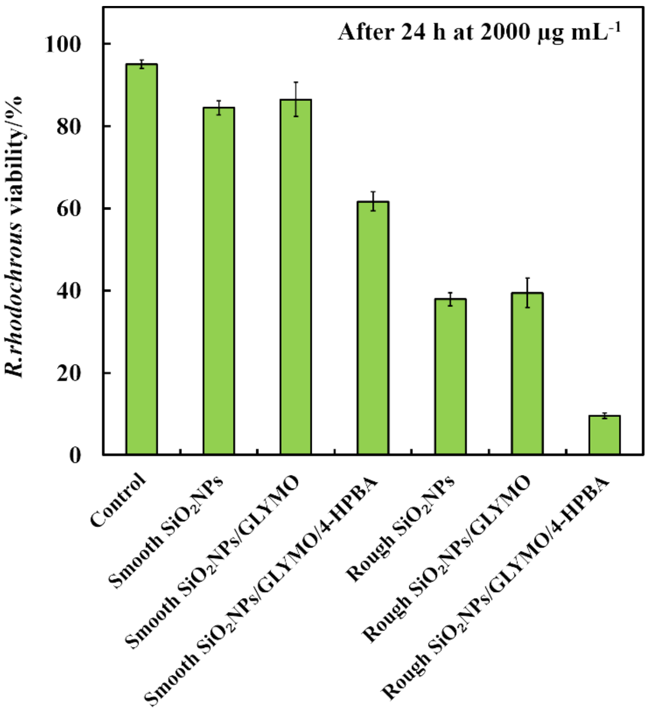

Figure 9. Comparison of the *R.rhodochrous* cell viability at 2000 µg mL^{-1} concentration of the bare and surface functionalized smooth and rough SiO_2NPs with GLYMO and 4-HPBA at 24 h of exposure time.

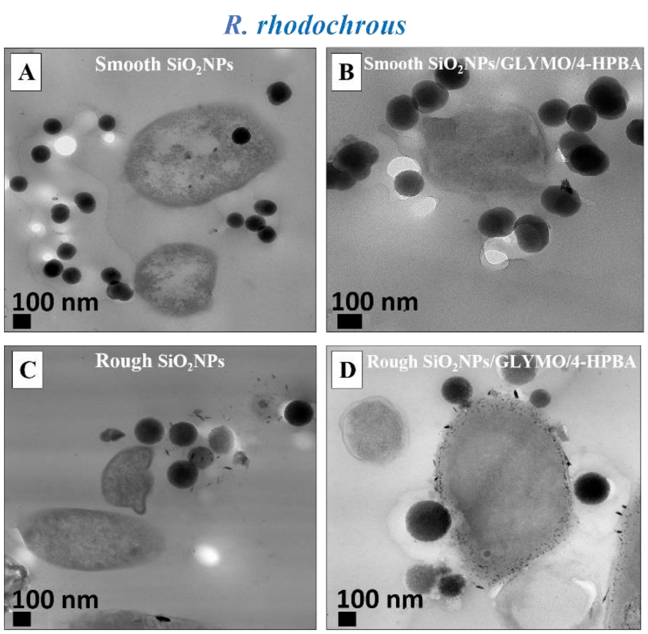

Figure 10. TEM images of epoxy resin-embedded and sectioned *R.rhodochrous* cells after 24 h exposure to the bare (A, C) and surface functionalized smooth (B) and rough (D) SiO_2NPs with GLYMO and 4-HPBA.

The effect is very similar to the antimicrobial action of CuONPs/GLYMO/4-HPBA which is strongly amplified compared with this of CuONPs/GLYMO.

This result implies that similar surface roughness copied from the original 'host' CuONPs combined with strongly adhesive interactions between the particles and the bacterial cell membrane leads to proportionate boost in their antimicrobial action compared with non-adhering nanoparticles at the same concentration (e.g. CuONPs/GLYMO or SiO_2NPs and SiO_2NPs/GLYMO). Note that the antimicrobial effect of the 'ghost' SiO_2NPs/GLYMO/4-HPBA is much higher than the smooth SiO_2NPs of the same functionalization (see Figure 9 and Figure 10). The TEM images confirm that the nanoparticles do not transfer into the bacteria cytoplasm, rather than accumulate on their cell walls. However, our estimates show that at the SiO_2NPs concentration of 500 µg mL^{-1} and a sample with 10^6 bacteria per mL, where the antibacterial effect of the ghost nanoparticles starts to manifests itself, the ratio between NPs and cells is nearly ~430,000, i.e. vastly in favor of the NPs. Hence not all NPs attach to the bacteria. The revealed mechanism of action, however, implies that even a single rough silica NP can pierce the bacterial cell wall. One may conclude that the 'ghost' SiO2NPs surface topology imposed through the templating process from the 'host' (CuONPs) greatly contributes to their antimicrobial action at the same particle size and surface chemistry. We also tested the antibacterial activity of 4-HPBA-functionalized rough SiO_2NPs and smooth SiO_2NPs on *E.coli* as shown in the added Figure S7 (ESI). The data in Figure S7 (ESI) show similar antibacterial trends to those observed with rough SiO_2NPs and smooth SiO_2NPs on *R.rhodochrous* (Figure 8A-8H). Since the 'ghost' SiO_2NPs act in the same way on both Gram-positive (*R.rhodochrous*) and Gram-negative (*E.coli*) bacterial, one can envisage that the suggested mechanism of antibacterial action seems to be universal.

Viability of HaCaT cells incubated with bare and HPBA-functionalized SiO2NPs. We tested the effect of HPBA-functionalized smooth and 'ghost' SiO_2NPs towards human keratinocytes as a proxy for human cells. Figure S6 (ESI) displays the cytotoxicity test of smooth and rough SiO_2NPs and SiO_2NPs/GLYMO/HPBA on HaCaT cells for up to 24 h of exposure. Note that the control sample of cells have lost a minor fraction of their viability over this period of time because of the depletion of the culture media. One can conclude that the NP does not measurably impact the HaCaT cell viability up to 2000 µg mL^{-1}. However, at these concentrations of the 'ghost' SiO_2NPs/GLYMO/4-HPBA, the impact on bacteria is very significant – see Figure 9. Therefore, one may conclude that the HPBA-functionalized 'ghost' SiO_2NPs shows excellent biocompatibility with these human skin cells. More research will have be conducted in the future on the NPs effects on various type of other cell lines. This functionality ('ghost' SiO_2NPs/GLYMO/HPBA) could have a potential topical application in wound care formulations.[33-34, 62-65]

CONCLUSIONS

We have explored how the imposition of similar surface morphology from antimicrobial nanoparticles made of CuO ('host') to one fabricated by their templating with a benign material like silica can yield nanoparticles of antimicrobial properties mimicking those of the host CuO nanoparticles. Here, we have developed a process to create a rough silica layer on the mesoporous CuONPs as templates that copies their surface roughness and morphology. TEM imaging confirmed that the silica was infused and coated the CuONPs. The diameter of the 'host/ghost' composite particles, CuONPs/SiO_2, was slightly increased, corresponding to a 25 ± 5 nm SiO_2 layer deposited on the CuONPs template, and the surface of CuONPs/SiO_2 acquired similar surface roughness as the original CuONPs ('host'). After removal of the CuO by treatment with HNO_3 and EDTA solutions we obtained surface-rough 'ghost' SiO_2NPs which mimic the 'host' CuONPs surface morphology. We functionalized the 'ghost' SiO_2NPs nanoparticles with 4-HPBA surface groups that allowed the 'ghost' SiO_2NPs particles to reversibly form covalent bonds with cis-diol groups from glycoproteins and carbohydrates expressed on the cell wall of bacteria. We demonstrated that by surface grafting of GLYMO and 4-HPBA on such surface-rough 'ghost' SiO_2NPs we can produce antimicrobial particle formulations which are several times more effective against bacteria compared to smooth SiO_2NPs at the same adhesive surface groups and particle concentration. Our tests also indicated that the anionic surface-rough SiO_2NPs/GLYMO/4-HPBA show much higher antibacterial activity than the bare smooth SiO_2NPs and the surface-rough but non-surface functionalized SiO_2NPs. This is explained by the strong covalent binding of the anionic surface-rough SiO_2NPs/GLYMO/4-HPBA to the bacterial cell membrane because of formation of boronic ester bonds between 4-HPBA groups on the functionalized nanoparticle surface and the diol groups from carbohydrates on the cell surface. Our results imply that the combination of adhesive particle-cell interactions with surface-rough morphology transferred from the 'host' CuONPs to the apparently benign SiO_2NPs by templating produced 'ghost' SiO_2NPs with significant 'host-intertied' antibacterial effect. One can say is that the surface roughness of the 'ghost' SiO_2NPs is on the same scale as the CuONPs templates and their particles sizes match closely. This, combined with similar surface functionalization with 4-HPBA yielded significant antimicrobial effect, although SiO_2 is usually benign to bacteria. Applying the same strategy to produce silica 'ghost' NPs with other antimicrobial nanoparticles like TiO_2NPs, ZnONPs, $Mg(OH)_2$NPs, etc. is also on our agenda but out of the scope of the present study. We also did experiments of incubation of the SiO_2NPs/GLYMO/4-HPBA with human keratinocytes which surprisingly showed no measurable cytotoxicity. This type of surface functionality showed good antibacterial activity. Hence, after surface grafting of GLYMO and 4-HPBA on the surface-rough SiO_2NPs could be used as an antibacterial agent.

AUTHOR INFORMATION

Corresponding Author

* Phone +44 1482 465660. Email: V.N.Paunov@hull.ac.uk

Author Contributions

The manuscript was written through contributions of all authors. All authors have given approval to the final version of the manuscript.

ACKNOWLEDGMENTS

A.F.H. thanks the Iraqi Government, the Higher Committee for Education Development of Iraq and the University of Babylon, Iraq for the financial support for his PhD study during the work on this project. The authors appreciated the technical help from Tony Sinclair and Ann Lowry at the University of Hull Microscopy Suite with the SEM and TEM sample preparation and imaging.

ASSOCIATED CONTENT

In the enclosed electronic supplementary information (ESI) we present the following additional data: (i) TEM images of SiO_2-coated CuONPs and a surface-rough SiO_2NPs; (ii) ζ-potential and particle size of CuONPs surface functionalized by SiO_2, GLYMO and 4-HPBA; (iii) ζ-potential and particle size of surface functionalized rough SiO_2NPs; (iv) Antibacterial activity of surface functionalized rough SiO_2NPs on *R.rhodochrous*; (v) Antibacterial activity of free GLYMO and 4-HPBA.

Funding Sources

A.F.H acknowledge funding of this work from the Higher Committee for Education Development of Iraq and the University of Babylon, Iraq.

ORCID

Ahmed F. Halbus: 0000-0001-9060-7073
Tommy S. Horozov: 0000-0001-8818-3750
Vesselin N. Paunov: 0000-0001-6878-1681

REFERENCES

(1) Palza, H. Antimicrobial Polymers with Metal Nanoparticles. *International journal of molecular sciences* **2015,** *16* (1), 2099-2116.

(2) Halbus, A. F.; Horozov, T. S.; Paunov, V. N. Strongly Enhanced Antibacterial Action of Copper Oxide Nanoparticles with Boronic Acid Surface Functionality. *ACS Applied Materials & Interfaces* **2019**, 11 (13), 2232–12243.

(3) Brayner, R.; Dahoumane, S. A.; Yepremian, C.; Djediat, C.; Meyer, M.; Coute, A.; Fievet, F. Zno Nanoparticles: Synthesis, Characterization, and Ecotoxicological Studies. *Langmuir* **2010,** *26* (9), 6522-8, DOI: 10.1021/la100293s.

(4) Zhang, H.; Chen, B.; Banfield, J. F. Particle Size and pH Effects on Nanoparticle Dissolution. *The Journal of Physical Chemistry C* **2010,** *114* (35), 14876-14884, DOI: 10.1021/jp1060842.

(5) Liu, J.; Aruguete, D. M.; Murayama, M.; Hochella Jr, M. F. Influence of Size and Aggregation on the Reactivity of an Environmentally and Industrially Relevant Nanomaterial (PbS). *Environmental science & technology* **2009,** *43* (21), 8178-8183.

(6) Zhang, Y.; Chen, Y.; Westerhoff, P.; Hristovski, K.; Crittenden, J. C. Stability of Commercial Metal Oxide Nanoparticles in Water. *Water research* **2008,** *42* (8), 2204-2212.

(7) Petosa, A. R.; Jaisi, D. P.; Quevedo, I. R.; Elimelech, M.; Tufenkji, N. Aggregation and Deposition of Engineered Nanomaterials in Aquatic Environments: Role of Physicochemical Interactions. *Environmental science & technology* **2010,** *44* (17), 6532-6549.

(8) Tiede, K.; Hassellöv, M.; Breitbarth, E.; Chaudhry, Q.; Boxall, A. B. Considerations for Environmental Fate and Ecotoxicity Testing to Support Environmental Risk Assessments for Engineered Nanoparticles. *Journal of Chromatography A* **2009,** *1216* (3), 503-509.

(9) Grassian, V. H. When Size Really Matters: Size-Dependent Properties and Surface Chemistry of Metal and Metal Oxide Nanoparticles in Gas and Liquid Phase Environments†. *The Journal of Physical Chemistry C* **2008,** *112* (47), 18303-18313.

(10) Abbas, Z.; Labbez, C.; Nordholm, S.; Ahlberg, E. Size-Dependent Surface Charging of Nanoparticles. *The Journal of Physical Chemistry C* **2008,** *112* (15), 5715-5723.

(11) Rao, C.; Kulkarni, G.; Thomas, P. J.; Edwards, P. P. Size-Dependent Chemistry: Properties of Nanocrystals. *Chemistry–A European Journal* **2002,** *8* (1), 28-35.

(12) Jolivet, J.-P.; Froidefond, C.; Pottier, A.; Chanéac, C.; Cassaignon, S.; Tronc, E.; Euzen, P. Size Tailoring of Oxide Nanoparticles by Precipitation in Aqueous Medium. A Semi-Quantitative Modelling. *Journal of Materials Chemistry* **2004,** *14* (21), 3281-3288.

(13) Zhao, Q.; Xie, T.; Peng, L.; Lin, Y.; Wang, P.; Peng, L.; Wang, D. Size-and Orientation-Dependent Photovoltaic Properties of ZnO Nanorods. *The Journal of Physical Chemistry C* **2007,** *111* (45), 17136-17145.

(14) McNeil, S. E. Nanotechnology for the Biologist. *Journal of Leukocyte Biology* **2005,** *78* (3), 585-594.

(15) Bian, S.-W.; Mudunkotuwa, I. A.; Rupasinghe, T.; Grassian, V. H. Aggregation and Dissolution of 4 nm ZnO Nanoparticles in Aqueous Environments: Influence of pH, Ionic Strength, Size, and Adsorption of Humic Acid. *Langmuir* **2011,** *27* (10), 6059-6068.

(16) Parham, S.; Wicaksono, D. H.; Bagherbaigi, S.; Lee, S. L.; Nur, H. Antimicrobial Treatment of Different Metal Oxide Nanoparticles: A Critical Review. *Journal of the Chinese Chemical Society* **2016,** *63* (4), 385-393.

(17) Fu, G.; Vary, P. S.; Lin, C.-T. Anatase TiO_2 Nanocomposites for Antimicrobial Coatings. *The Journal of Physical Chemistry B* **2005,** *109* (18), 8889-8898.

(18) Makhluf, S.; Dror, R.; Nitzan, Y.; Abramovich, Y.; Jelinek, R.; Gedanken, A. Microwave-Assisted Synthesis of Nanocrystalline MgO and Its Use as a Bacteriocide. *Advanced Functional Materials* **2005,** *15* (10), 1708-1715.

(19) Halbus, A. F.; Horozov, T. S.; Paunov, V. N. Colloid Particle Formulations for Antimicrobial Applications. *Advances in colloid and interface science* **2017,** *249*, 134-148.

(20) Kaweeteerawat, C.; Ivask, A.; Liu, R.; Zhang, H.; Chang, C. H.; Low-Kam, C.; Fischer, H.; Ji, Z.; Pokhrel, S.; Cohen, Y. Toxicity of Metal Oxide Nanoparticles in Escherichia Coli Correlates with Conduction Band and Hydration Energies. *Environmental science & technology* **2015,** *49* (2), 1105-1112.

(21) Al-Awady, M. J.; Greenway, G. M.; Paunov, V. N. Nanotoxicity of Polyelectrolyte-Functionalized Titania Nanoparticles towards Microalgae and Yeast: Role of the Particle Concentration, Size and Surface Charge. *RSC Advances* **2015,** *5* (46), 37044-37059.

(22) Reddy, K. M.; Feris, K.; Bell, J.; Wingett, D. G.; Hanley, C.; Punnoose, A. Selective Toxicity of Zinc Oxide Nanoparticles to Prokaryotic and Eukaryotic Systems. *Applied physics letters* **2007,** *90* (21), 213902.

(23) Lee, C.; Kim, J. Y.; Lee, W. I.; Nelson, K. L.; Yoon, J.; Sedlak, D. L. Bactericidal Effect of Zero-Valent Iron Nanoparticles on Escherichia Coli. *Environmental science & technology* **2008,** *42* (13), 4927-4933.

(24) Yoon, K.-Y.; Byeon, J. H.; Park, J.-H.; Hwang, J. Susceptibility Constants of Escherichia Coli and Bacillus Subtilis to Silver and Copper Nanoparticles. *Science of the Total Environment* **2007,** *373* (2-3), 572-575.

(25) Sahoo, P.; Murthy, P. S.; Dhara, S.; Venugopalan, V.; Das, A.; Tyagi, A. Probing the Cellular Damage in Bacteria Induced by Gan Nanoparticles Using Confocal Laser Raman Spectroscopy. *Journal of nanoparticle research* **2013,** *15* (8), 1841.

(26) Singh, G.; Joyce, E. M.; Beddow, J.; Mason, T. J. Evaluation of Antibacterial Activity of ZnO Nanoparticles Coated Sonochemically onto Textile Fabrics. *The Journal of Microbiology, Biotechnology and Food Sciences* **2012,** *2* (1), 106.

(27) Goodman, C. M.; McCusker, C. D.; Yilmaz, T.; Rotello, V. M. Toxicity of Gold Nanoparticles Functionalized with Cationic and Anionic Side Chains. *Bioconjugate chemistry* **2004,** *15* (4), 897-900.

(28) Silva, T.; Pokhrel, L. R.; Dubey, B.; Tolaymat, T. M.; Maier, K. J.; Liu, X. Particle Size, Surface Charge and Concentration Dependent Ecotoxicity of Three Organo-Coated Silver Nanoparticles: Comparison Between General Linear Model-Predicted and Observed Toxicity. *Science of the total environment* **2014,** *468*, 968-976.

(29) Simon-Deckers, A.; Loo, S.; Mayne-L'hermite, M.; Herlin-Boime, N.; Menguy, N.; Reynaud, C.; Gouget, B.; Carriere, M. Size-, Composition-and Shape-Dependent Toxicological Impact of Metal Oxide Nanoparticles and Carbon Nanotubes Toward Bacteria. *Environmental science & technology* **2009,** *43* (21), 8423-8429.

(30) Xiao, X.; Montaño, G. A.; Edwards, T. L.; Allen, A.; Achyuthan, K. E.; Polsky, R.; Wheeler, D. R.; Brozik, S. M. Surface Charge Dependent Nanoparticle Disruption and Deposition of Lipid Bilayer Assemblies. *Langmuir* **2012,** *28* (50), 17396-17403.

(31) Roiter, Y.; Ornatska, M.; Rammohan, A. R.; Balakrishnan, J.; Heine, D. R.; Minko, S. Interaction of Lipid Membrane with Nanostructured Surfaces. *Langmuir* **2009,** *25* (11), 6287-6299.

(32) Mathelié-Guinlet, M.; Béven, L.; Moroté, F.; Moynet, D.; Grauby-Heywang, C.; Gammoudi, I.; Delville, M.-H.; Cohen-Bouhacina, T. Probing the Threshold of Membrane Damage and Cytotoxicity Effects Induced by Silica Nanoparticles in Escherichia Coli Bacteria. *Advances in colloid and interface science* **2017,** *245*, 81-91.

(33) Al-Awady, M. J.; Fauchet, A.; Greenway, G. M.; Paunov, V. N. Enhanced Antimicrobial Effect of Berberine in Nanogel Carriers with Cationic Surface Functionality. *Journal of Materials Chemistry B* **2017,** 5 (38), 7885-7897.

(34) Al-Awady, M. J.; Weldrick, P. J.; Hardman, M. J.; Greenway, G. M.; Paunov, V. N. Amplified Antimicrobial Action of Chlorhexidine Encapsulated in PDAC-Functionalized Acrylate

Copolymer Nanogel Carriers. *Materials Chemistry Frontiers* **2018**, *2*, 2032-2044.
(35) Al-Obaidy, S. S.; Greenway, G. M.; Paunov, V. N. Dual-Functionalised Shellac Nanocarriers Give a Super-Boost of the Antimicrobial Action of Berberine. *Nanoscale Advances* **2019**, *1*, 858–872.
(36) Tan, W.; Wang, K.; He, X.; Zhao, X. J.; Drake, T.; Wang, L.; Bagwe, R. P. Bionanotechnology Based on Silica Nanoparticles. *Medicinal research reviews* **2004**, *24* (5), 621-638.
(37) Wang, Y.; Zhao, Q.; Han, N.; Bai, L.; Li, J.; Liu, J.; Che, E.; Hu, L.; Zhang, Q.; Jiang, T. Mesoporous Silica Nanoparticles in Drug Delivery and Biomedical Applications. *Nanomedicine: Nanotechnology, Biology and Medicine* **2015**, *11* (2), 313-327.
(38) Pham, M. T.; Van Nguyen, T.; Thi, T. D. V.; Thi, H. L. N.; Tong, K. T.; Tran, T. T.; Chu, V. H.; Brochon, J.-C.; Tran, H. N. Synthesis, Photophysical Properties and Application of Dye Doped Water Soluble Silica-Based Nanoparticles to Label Bacteria *E. coli* O157: H7. *Advances in Natural Sciences: Nanoscience and Nanotechnology* **2012,** *3* (4), 045013.
(39) Guo, Z.; Xue, J.; Liu, T.; Song, X.; Shen, Y.; Wu, H. Antibacterial Mechanisms of Silica/Polydopamine/Silver Nanoparticles Against Gram Positive and Gram Negative Bacteria. *Micro & Nano Letters* **2014,** *9* (3), 210-214.
(40) Molina-Manso, D.; Manzano, M.; Doadrio, J. C.; Del Prado, G.; Ortiz-Pérez, A.; Vallet-Regí, M.; Gómez-Barrena, E.; Esteban, J. Usefulness of SBA-15 Mesoporous Ceramics as a Delivery System for Vancomycin, Rifampicin and Linezolid: a Preliminary Report. *International journal of antimicrobial agents* **2012,** *40* (3), 252-256.
(41) Yu, E.; Galiana, I.; Martínez-Máñez, R.; Stroeve, P.; Marcos, M. D.; Aznar, E.; Sancenón, F.; Murguía, J. R.; Amorós, P. Poly (N-Isopropylacrylamide)-Gated Fe3O4/SiO2 Core Shell Nanoparticles with Expanded Mesoporous Structures for the Temperature Triggered Release of Lysozyme. *Colloids and Surfaces B: Biointerfaces* **2015,** *135*, 652-660.
(42) Ruiz-Rico, M.; Fuentes, C.; Pérez-Esteve, É.; Jiménez-Belenguer, A. I.; Quiles, A.; Marcos, M. D.; Martínez-Máñez, R.; Barat, J. M. Bactericidal Activity of Caprylic Acid Entrapped in Mesoporous Silica Nanoparticles. *Food Control* **2015,** *56*, 77-85.
(43) Du, X.; He, J. A Self-Templated Etching Route to Surface-Rough Silica Nanoparticles for Superhydrophobic Coatings. *ACS applied materials & interfaces* **2011,** *3* (4), 1269-1276.
(44) De Silva, A. P.; Gunaratne, H. N.; Gunnlaugsson, T.; Huxley, A. J.; McCoy, C. P.; Rademacher, J. T.; Rice, T. E. Signaling Recognition Events with Fluorescent Sensors and Switches. *Chemical reviews* **1997,** *97* (5), 1515-1566.
(45) Lacina, K.; Skládal, P.; James, T. D. Boronic Acids for Sensing and Other Applications-a Mini-Review of Papers Published in 2013. *Chemistry Central Journal* **2014,** *8* (1), 60.
(46) Trippier, P. C.; McGuigan, C. Boronic Acids in Medicinal Chemistry: Anticancer, Antibacterial and Antiviral Applications. *MedChemComm* **2010,** *1* (3), 183-198.
(47) Yan, J.; Springsteen, G.; Deeter, S.; Wang, B. The Relationship Among pKa, pH, and Binding Constants in the Interactions Between Boronic Acids and Diols—it is not as Simple as it Appears. *Tetrahedron* **2004,** *60* (49), 11205-11209.
(48) Kuzimenkova, M.V.; Ivanov, A. E.; Thammakhet, C.; Mikhalovska, L. I.; Galaev, I. Y.; Thavarungkul, P.; Kanatharana, P.; Mattiasson, B. Optical Responses, Permeability and Diol-Specific Reactivity of Thin Polyacrylamide Gels Containing Immobilized Phenylboronic Acid. *Polymer* **2008,** *49* (6), 1444-1454.
(49) Lau, O.-W.; Shao, B.; Lee, M. T. Affinity Mass Sensors: Determination of Fructose. *Analytica chimica acta* **2000,** *403* (1-2), 49-56.
(50) Ertl, P.; Mikkelsen, S. R. Electrochemical Biosensor Array for the Identification of Microorganisms Based on Lectin–Lipopolysaccharide Recognition. *Analytical chemistry* **2001,** *73* (17), 4241-4248.
(51) Wannapob, R.; Kanatharana, P.; Limbut, W.; Numnuam, A.; Asawatreratanakul, P.; Thammakhet, C.; Thavarungkul, P. Affinity Sensor Using 3-Aminophenylboronic Acid for Bacteria Detection. *Biosensors and Bioelectronics* **2010,** *26* (2), 357-364.
(52) Liu, S.; Wollenberger, U.; Halámek, J.; Leupold, E.; Stöcklein, W.; Warsinke, A.; Scheller, F. W. Affinity Interactions between Phenylboronic Acid-Carrying Self-Assembled Monolayers and Flavin Adenine Dinucleotide or Horseradish Peroxidase. *Chemistry–A European Journal* **2005,** *11* (14), 4239-4246.
(53) Elmas, B.; Onur, M.; Şenel, S.; Tuncel, A. Temperature Controlled RNA Isolation by N-Isopropylacrylamide–Vinylphenyl Boronic Acid Copolymer Latex. *Colloid and Polymer Science* **2002,** *280* (12), 1137-1146.
(54) DiCesare, N.; Lakowicz, J. R. Evaluation of Two Synthetic Glucose Probes for Fluorescence-Lifetime-Based Sensing. *Analytical biochemistry* **2001,** *294* (2), 154-160.
(55) Zeng, W.; Wang, Z.; Qian, X.-F.; Yin, J.; Zhu, Z.-K. ZnO Clusters in Situ Generated Inside Mesoporous Silica. *Materials research bulletin* **2006,** *41* (6), 1155-1159.
(56) El-Nahhal, I. M.; Salem, J. K.; Kuhn, S.; Hammad, T.; Hempelmann, R.; Al Bhaisi, S. Synthesis & Characterization of Silica Coated and Functionalized Silica Coated Zinc Oxide Nanomaterials. *Powder Technology* **2016,** *287*, 439-446.
(57) El-Nahhal, I. M.; Salem, J. K.; Kuhn, S.; Hammad, T.; Hempelmann, R.; Al Bhaisi, S. Synthesis and Characterization of Silica-, Meso-Silica-and Their Functionalized Silica-Coated Copper Oxide Nanomaterials. *Journal of Sol-Gel Science and Technology* **2016,** *79* (3), 573-583.
(58) Grasset, F.; Saito, N.; Li, D.; Park, D.; Sakaguchi, I.; Ohashi, N.; Haneda, H.; Roisnel, T.; Mornet, S.; Duguet, E. Surface Modification of Zinc Oxide Nanoparticles by Aminopropyltriethoxysilane. *Journal of Alloys and Compounds* **2003,** *360* (1), 298-311.
(59) Cunningham, V. J.; Alswieleh, A. M.; Thompson, K. L.; Williams, M.; Leggett, G. J.; Armes, S. P.; Musa, O. M. Poly(glycerol monomethacrylate)–Poly(benzyl methacrylate) Diblock Copolymer Nanoparticles via RAFT Emulsion Polymerization: Synthesis, Characterization, and Interfacial Activity. *Macromolecules* **2014,** *47* (16), 5613-5623, DOI: 10.1021/ma501140h.
(60) Zhang, D.; Thompson, K. L.; Pelton, R.; Armes, S. P. Controlling Deposition and Release of Polyol-Stabilized Latex on Boronic Acid-Derivatized Cellulose. *Langmuir* **2010,** *26* (22), 17237-17241.
(61) Pelton, R.; Zhang, D.; Thompson, K. L.; Armes, S. P. Borate Binding to Polyol-Stabilized Latex. *Langmuir* **2011,** *27* (6), 2118-2123.
(62) Penders, J.; Stolzoff, M.; Hickey, D. J.; Andersson, M.; Webster, T. J. Shape-Dependent Antibacterial Effects of Non-Cytotoxic Gold Nanoparticles. *International journal of nanomedicine* **2017,** *12*, 2457-2468.
(63) Halbus, A. F.; Horozov, T. S.; Paunov, V. N. Self-Grafting Copper Oxide Nanoparticles Show a Strong Enhancement of their Anti-Algal and Anti-Yeast Action, *Nanoscale Advances*, **2019**, 1 (6), 2323–2336.

(64) Halbus, A.F.; Horozov, T.S.; Paunov, V.N.; Controlling the Antimicrobial Action of Surface Modified Magnesium Hydroxide Nanoparticles, *Biomimetics*, 2019, 4 (2), 41.1-20.
(65) Weldrick, P.J.; Iveson, S.; Hardman, M.J.; Paunov, V.N. Breathing New Life into Old Antibiotics: Overcoming Antibacterial Resistance by Antibiotic-Loaded Nanogel Carriers with Cationic Surface Functionality, *Nanoscale*, **2019**, 11 (21), 10472-10485.

TOC graphics